

# Practical short-term voltage stability index based on voltage curves: definition, verification and case studies

 ISSN 1751-8687  
 Received on 19th November 2017  
 Revised 30th May 2018  
 Accepted on 10th August 2018  
 E-First on 20th September 2018  
 doi: 10.1049/iet-gtd.2018.5725  
 www.ietdl.org

 Wenlu Zhao<sup>1</sup>, Qinglai Guo<sup>1</sup>, Hongbin Sun<sup>1</sup> ✉, Huaichang Ge<sup>1</sup>, Haifeng Li<sup>2</sup>
<sup>1</sup>Electrical Engineering, Tsinghua University, Haidian District, Beijing, People's Republic of China

<sup>2</sup>Jiangsu Electrical Company, Gulou District, Nanjing, People's Republic of China

✉ E-mail: shb@mail.tsinghua.edu.cn

**Abstract:** Short-term voltage stability (SVS) is a serious issue in modern power systems. In China, the East China Power Network is especially vulnerable to short-term voltage instability due to its increasing dependence on electrical power from external through high-voltage direct current (HVDC) transmission lines. To study the SVS, a criterion/index is first required to evaluate the SVS of power systems. However, the currently used practical criteria cannot effectively evaluate the influence of controlling strategies (such as regulating dynamic VAR reservation) of power systems. Therefore, a practical and continuous SVS index (SVSI) based on voltage curves is proposed in this study. The proposed SVSI can quantify the extent of SVS in power systems, thus can be used in the optimisation target of preventive control for improving the SVS of power systems. Moreover, the SVSI consists of three components, and each component reflects a feature of the voltage curve in terms of SVS. The SVSI is essentially a model-free method for assessing the SVS of power systems, so it is robust. Three verifying cases and one application case are presented to show the validity of the SVSI and the feasibility of the SVSI in practical applications.

## 1 Introduction

Voltage stability is important for the steady operation of power systems. Historically, several blackouts have been induced by voltage instability, such as the North American blackout in August 2003 [1]. However, modern power systems are operating under more stressed conditions due to increasing load demands and increasing electricity exchange between regional grids. Additionally, their dynamic responses are more complicated with the increasing use of induction motor loads, electronically controlled loads, high-voltage direct current (HVDC) transmission systems and so on. Therefore, power systems are more vulnerable to short-term voltage stability (SVS) problems [2].

The SVS problem of the power systems in China is significant because long-distance transmission is required to deliver electrical power from the west to the east [3–6]. For example, under a typical operating mode in summer, the East China Power Network (ECPN) receives over 44,000 MW of electrical power (16% of its total load demand) from external power grids through HVDC transmission lines. The SVS problem in the Yangtze River Delta is especially significant due to its increasing dependence on electrical power from external and lack of reactive power reserves. Therefore, the SVS of power systems is a significant and practical problem that should be taken seriously.

To evaluate the SVS of power systems, a criterion/index is first required. Currently, the indices for evaluating SVS can be divided into two categories: indices based on physical/mathematical

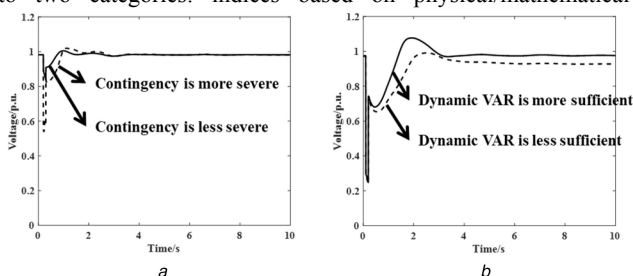


**Fig. 1** Voltage curves of a same bus

(a) Corresponding to two contingencies, (b) Corresponding to two dynamic VAR reservations

theories (such as the transient energy function [7–10] and the non-linear dynamic approach [11, 12]) and indices based on voltage curves. Indices based on physical/mathematical theories can explain the mechanism of SVS, but they are difficult to apply to large-scale power systems (such as the ECPN). So most of the practical criteria for evaluating SVS are based on voltage curves.

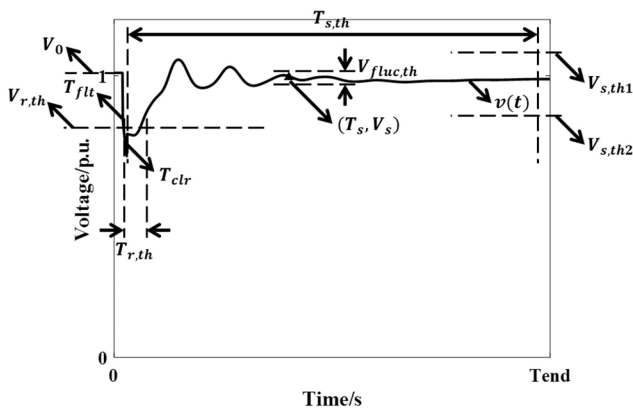
Some practical SVS criteria are presented in [13–18]. These criteria can determine whether the power system is stable or not, but they cannot differentiate the extent of SVS of the power system under different operating status. For instance, according to the SVS criterion of State Grid Corporation of China (SGCC) [17], the voltage curves in Fig. 1 are both stable, so they are equivalent according to the practical SVS criteria. However, apparently the SVS of the two black curves in Figs. 1a and b is better than those of the two red curves. So the contingency corresponding to the red curve in Fig. 1a is more severe, and the allocation of dynamic VAR corresponding to the black curve in Fig. 1b shows some improvement. These above-mentioned practical SVS criteria cannot effectively assess the influence of controlling strategies (such as regulating dynamic VAR reservation) of power systems, thus they cannot be used in the optimisation target of the control strategies to improve the SVS of power systems.

To improve the SVS of power systems, two ways are usually utilised: the emergency control [19] which is utilised to the post-contingency system and the preventive control [20, 21] which is utilised to the pre-contingency system. In the preventive control, usually all the anticipated contingencies are considered. So the preventive control problem for improving the SVS of power system is essentially a constrained optimisation problem. In order to ensure the robustness of the power system, a margin of SVS is usually necessary to be included in the optimisation target of preventive control. Therefore, a continuous index is required to describe the margin of SVS, but the practical discrete criteria/index cannot meet this requirement.

In view of the limitations of the practical SVS criteria, a continuous index for evaluating SVS and describing the margin of SVS is required. Analysis of SVS based on voltage curves is the most reliable way in practice, and is widely used in many power grids around the world. However, voltage curves cannot be used directly as an index for evaluating SVS. Therefore, an SVS index (SVSI) based on voltage curves will be proposed in this paper,

**Table 1** Parameters used in the definition of SVSI

Parameter	Definition
$v(t)$	voltage curve during transient process
$V_0$	pre-contingency steady-state voltage
$T_{flt}$	time instant when contingency starts
$T_{clr}$	time instant when contingency is cleared
$T_{end}$	time instant at the end of $v(t)$
$T_{r,th}$	time duration threshold for continuous low voltage in transient process, used in calculating $SVSI_r$
$V_{r,th}$	low voltage threshold in transient process, used in calculating $SVSI_r$
$T_{s,th}$	time duration threshold to reach post-contingency steady state, used in calculating $SVSI_s$
$V_{s,th1}$	voltage upper limit in steady state, used in calculating $SVSI_s$
$V_{s,th2}$	voltage lower limit in steady state, used in calculating $SVSI_s$
$V_{fluc,th}$	voltage fluctuation limit in steady state, used in calculating $T_s$
$T_s$	time instant when $v(t)$ reaches the post-contingency steady state, used in calculating $SVSI_s$
$V_s$	post-contingency steady-state voltage, used in calculating $SVSI_s$
$A_s$	parameter, used in calculating $SVSI_s$
$T_l$	parameter, used in calculating $SVSI_l$
$T_{spl}$	sampling step of $v(t)$ , used in calculating $SVSI_l$

**Fig. 2** Schematic of a voltage curve and the relevant parameters of SVSI

which can extract the key features of voltage curves in terms of SVS.

Previously, several practical and quantitative indices for the studies of SVS have been proposed, which have given us inspirations for constructing the SVSI in this paper. Indices which describe the integration of voltage deviation over time are used in [22–25], and indices which describe the time span that voltage violates limits are used in [26, 27]. These indices can satisfy their research requirements, respectively, but they cannot comprehensively evaluate the extent/margin of SVS.

Compared to the practical criteria and the indices used in previous studies, the SVSI proposed in this paper has four key features. First, the SVSI is calculated only based on voltage curves. The voltage curves can be obtained through numerical simulation and so on. Second, the SVSI is continuous, thus it can be used in the optimisation target of the preventive control. Third, the SVSI considers three aspects of the voltage curves in terms of SVS, the weight among them can be modified according to the focus of preventive control. Lastly, the index realises the digitalisation of voltage curves and can give a comprehensive evaluation of extent/margin of SVS, thus it can be used in practical issues such as identifying weak SVS regions. The definition, analysis, verification and application of the SVSI are presented in the following sections.

The arrangement of this paper is as follows. The definition and analysis of the SVSI is presented in Section 2. The verifying case studies are shown in Section 3. An application case study is shown in Section 4. The conclusions are drawn in Section 5. The acknowledgments are in Section 6.

## 2 SVSI based on voltage curves

### 2.1 Definition of parameters

Some parameters are required to define the SVSI, which are presented in Table 1.

A schematic of a voltage curve and the parameters is shown in Fig. 2. The detailed description of each parameter will be stated in the definition of SVSI.

### 2.2 $SVSI_r$ : describe the ability of transient voltage restoration

In this paper, the transient voltage restoration is regarded as the process that bus voltage restores from low voltage state caused by contingencies.

Before defining  $SVSI_r$ , the low voltage threshold and low voltage duration threshold are required to be identified, i.e.  $V_{r,th}$  and  $T_{r,th}$ . In practice, according to the WECC Planning Standards [13, 14], the voltage dip should not exceed 20% for more than 20 cycles at load buses under an event resulting in the loss of a single element.

The definition of  $SVSI_r$  is

$$S_{T_{span}} = \left\{ \{t_1, t_2\} \left| \begin{array}{l} v(t_1) = v(t_2) = V_{r,th}, 0 \leq t_1 < t_2 \leq T_{end}; \\ \forall t \in [t_1, t_2], v(t) < V_{r,th} \end{array} \right. \right\} \quad (1)$$

$$T_{span,max} = \begin{cases} \max(t_2 - t_1), \{t_1, t_2\} \in S_{T_{span}} & \text{if } S_{T_{span}} \neq \emptyset \\ 0 & \text{if } S_{T_{span}} = \emptyset \end{cases} \quad (2)$$

$$SVSI_r = T_{span,max} / T_{r,th} \quad (3)$$

There is only one key variable to calculate  $SVSI_r$ , i.e.  $T_{span,max}$ .  $T_{span,max}$  is the length of the longest time duration that  $v(t)$  persists below  $V_{r,th}$ , and  $SVSI_r$  is the value of  $T_{span,max}$  divided by  $T_{r,th}$ . The range of  $SVSI_r$  is  $[0, +\infty)$ . The ability of transient voltage restoration becomes worse as  $SVSI_r$  increases. When  $SVSI_r$  equals to 1, the ability of transient voltage restoration is critical. A schematic of  $SVSI_r$  is shown in Fig. 3.

Apparently, the ability of transient restoration of the voltage curve is better in Fig. 3a compared to the ability of transient restoration of the voltage curve in Fig. 3b. The  $SVSI_r$  of the voltage curve is smaller in Fig. 3a compared to the  $SVSI_r$  of the voltage curve in Fig. 3b. Therefore, the smaller is the value of  $SVSI_r$ , the better is the ability of transient restoration of the voltage curve.

$SVSI_r$  is closely related to the response of dynamic elements at low voltage. For instance, if the voltage stays below a low voltage threshold for more than a time duration threshold, it may cause stalling of induction motors, commutation failure of DC converter stations and so on.

The ability of transient voltage restoration is closely related to reactive power, so we can analyse the impact of dynamic elements on  $SVSI_r$  in terms of reactive power. During transient voltage restoration, the induction motors and the HVDCs consume a massive amount of reactive power and thus threaten the SVS of the power system. On the contrary, the over-excitation of generators and the dynamic VARs (such as the static synchronous compensators (STATCOMs) and the static VAR compensators (SVCs)), can rapidly generate reactive power to support the voltage stability of the power system.

So to decrease  $SVSI_r$  and improve the ability of transient voltage restoration, we can focus on modification of the dynamic response of induction motor loads, adjustment of the controllers of the HVDC transmission lines, optimisation of the AVR parameters, increasing the reservation of dynamic VARs and so on.

### 2.3 SVSI<sub>s</sub>: describe the ability to reach post-contingency steady state

In this paper, the ability to reach post-contingency steady state considers both the post-contingency steady-state voltage and the time to reach post-contingency steady state.

Before defining SVSI<sub>s</sub>, the post-contingency steady-state voltage and the time to reach steady state are required to be identified, i.e.  $V_s$  and  $T_s$ . In order to calculate  $V_s$  and  $T_s$ , we need to identify the voltage fluctuation threshold at steady state, i.e.  $V_{fluc,th}$ . The fluctuation of  $v(t)$  will not exceed  $V_{fluc,th}$  after  $T_s$ , and  $V_s$  is the average value of  $v(t)$  after  $T_s$ . Additionally, in order to assess the post-contingency steady state, the upper limit and lower limit of steady-state voltage together with the time limit to reach steady state are also required to be identified, i.e.  $V_{s,th1}$ ,  $V_{s,th2}$  and  $T_{s,th}$ .

In practice, according to the SVS criterion of SGCC [17], the voltage should recover to 0.8 p.u. in 10 s after the contingency has been cleared; according to the voltage constraint of steady-state operation in China [28], the steady-state voltage should not exceed 1.1 p.u.; according to the voltage fluctuation constraint of steady-state operation in China [29], the voltage fluctuation should not exceed 0.01 p.u.

The definition of SVSI<sub>s</sub> is

SVSI<sub>s</sub> =

$$\left\{ \begin{array}{ll} -\frac{V_s - V_{s,th2}}{V_{s,th2}} \times \frac{(A_s T_{s,th})^2 - T_{s,th}^2}{(A_s T_{s,th})^2 - T_s^2} + 1, & 0 \leq V_s < V_{s,th2} \\ \frac{V_s - V_{s,th2}}{V_0 - V_{s,th2}} \times \frac{T_s - T_{s,th}}{T_{s,th}} + 1, & V_{s,th2} \leq V_s < V_0 \\ \frac{V_s - V_{s,th1}}{V_0 - V_{s,th1}} \times \frac{T_s - T_{s,th}}{T_{s,th}} + 1, & V_0 \leq V_s < V_{s,th1} \\ \frac{V_s - V_{s,th1}}{V_{s,th1}} \times \frac{(A_s T_{s,th})^2 - T_{s,th}^2}{(A_s T_{s,th1})^2 - T_s^2} + 1, & V_{s,th1} \leq V_s \end{array} \right. \quad (4)$$

There are two key variables to calculate SVSI<sub>s</sub>, i.e.  $V_s$  and  $T_s$ . If  $v(t)$  cannot reach a post-contingency steady state, then  $V_s$  is set to be  $v(T_{s,th})$  and  $T_s$  is set to be the  $T_{s,th}$ .  $A_s$  is a constant  $>1$ , so that  $A_s T_{s,th}$  is greater than  $T_{s,th}$ . The three critical voltage values (i.e.  $V_{s,th2}$ ,  $V_0$  and  $V_{s,th1}$ ) and one critical time instant (i.e.  $T_{end}$ ) are regarded as the boundaries to determine the status of post-contingency steady state, so the definition of SVSI<sub>s</sub> consists of four parts (i.e.  $0 \leq V_s < V_{s,th2}$ ,  $V_{s,th2} \leq V_s < V_0$ ,  $V_0 \leq V_s < V_{s,th1}$  and  $V_{s,th1} \leq V_s$ ).

The range of SVSI<sub>s</sub> is  $[0, +\infty)$ . The status of post-contingency steady-state becomes worse as SVSI<sub>s</sub> increases. When SVSI equals to 1, the status of post-contingency steady state is critical. Additionally, the range of SVSI<sub>s</sub> is  $(1, 2]$  when  $0 \leq V_s < V_{s,th2}$ , is  $(0, 1]$  when  $V_{s,th2} \leq V_s < V_0$ , is  $[0, 1)$  when  $V_0 \leq V_s < V_{s,th1}$ , is  $[1, +\infty)$  when  $V_{s,th1} \leq V_s$ . A schematic of SVSI<sub>s</sub> is shown in Fig. 4.

The colourful line series in Fig. 4a are the contours of SVSI<sub>s</sub>, and the value on the contours are their corresponding SVSI<sub>s</sub>. The contour whose corresponding SVSI<sub>s</sub> equals to 1 is regarded as the boundary of stability according to the definition of  $V_{s,th1}$ ,  $V_{s,th2}$  and  $T_{s,th}$ . Referring to the practical operating experiences, if a  $v(t)$  reaches the post-contingency steady state rapidly and the deviation of the post-contingency steady state and pre-contingency steady state is small, then its ability to reach post-contingency steady state is good. So the contours of SVSI<sub>s</sub> are all concave to point  $(0, V_s)$ .

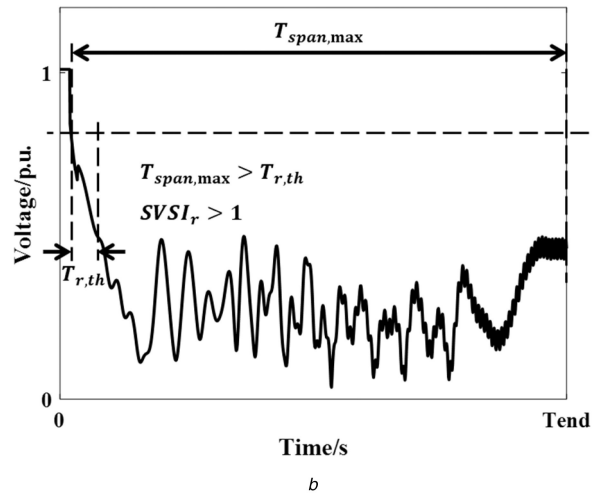
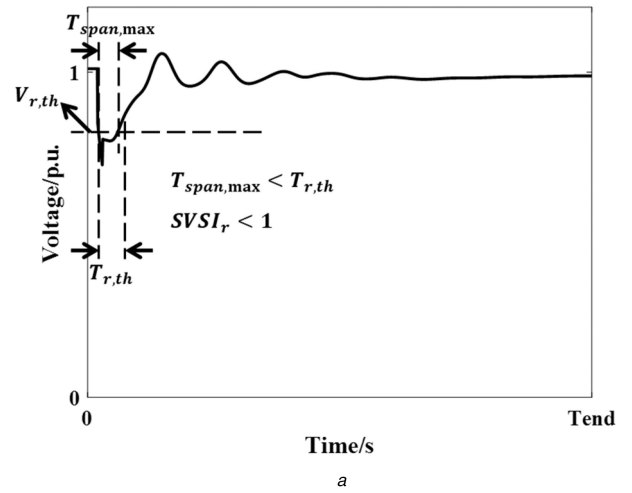


Fig. 3 Schematic of SVSI<sub>r</sub>

(a) SVSI<sub>r</sub> under a voltage stable case, (b) SVSI<sub>r</sub> under a voltage unstable case.

Apparently, in Fig. 4c, the steady state of the black curve is considerably better than the steady state of the blue curve (actually, the blue curve never reaches a steady-state after the contingency has been cleared). Meanwhile, the SVSI<sub>s</sub> of the black curve is smaller compared to the SVSI<sub>s</sub> of the blue curve. So the smaller is the value of SVSI<sub>s</sub>, the better is the status of the post-contingency steady state of a voltage curve.

SVSI<sub>s</sub> is closely related to the post-contingency topology and the stability status after the contingency has been cleared. For instance, if a transmission line is tripped after the contingency has been cleared, then  $V_s$  may be smaller than  $V_0$ , and thus the SVSI<sub>s</sub> will be larger than 0. Besides, if the voltage is unstable after the contingency has been cleared, then the SVSI<sub>s</sub> will be larger than 1.

So to decrease SVSI<sub>s</sub> and improve the status of post-contingency steady state, we can focus on the modification of the post-contingency topology, such as under-voltage load-shedding, cut-off generators and so on.

### 2.4 SVSI<sub>s</sub>: describe the level of transient voltage oscillation

In this paper, the level of transient voltage oscillation is described by the convergence of voltage curves.

The Lyapunov exponents can be considered as a description of the eigenvalues of the non-linear systems, and can provide the divergence or convergence information of adjacent system trajectories. In particular, if the maximum Lyapunov exponent of the system is negative, then the adjacent trajectories of the system converge, and thus the dynamic response of the system is stable. Otherwise, the dynamic response of the system is unstable.

For a single trajectory, the Lyapunov exponent can be calculated by assessing the distance between the actual trajectory

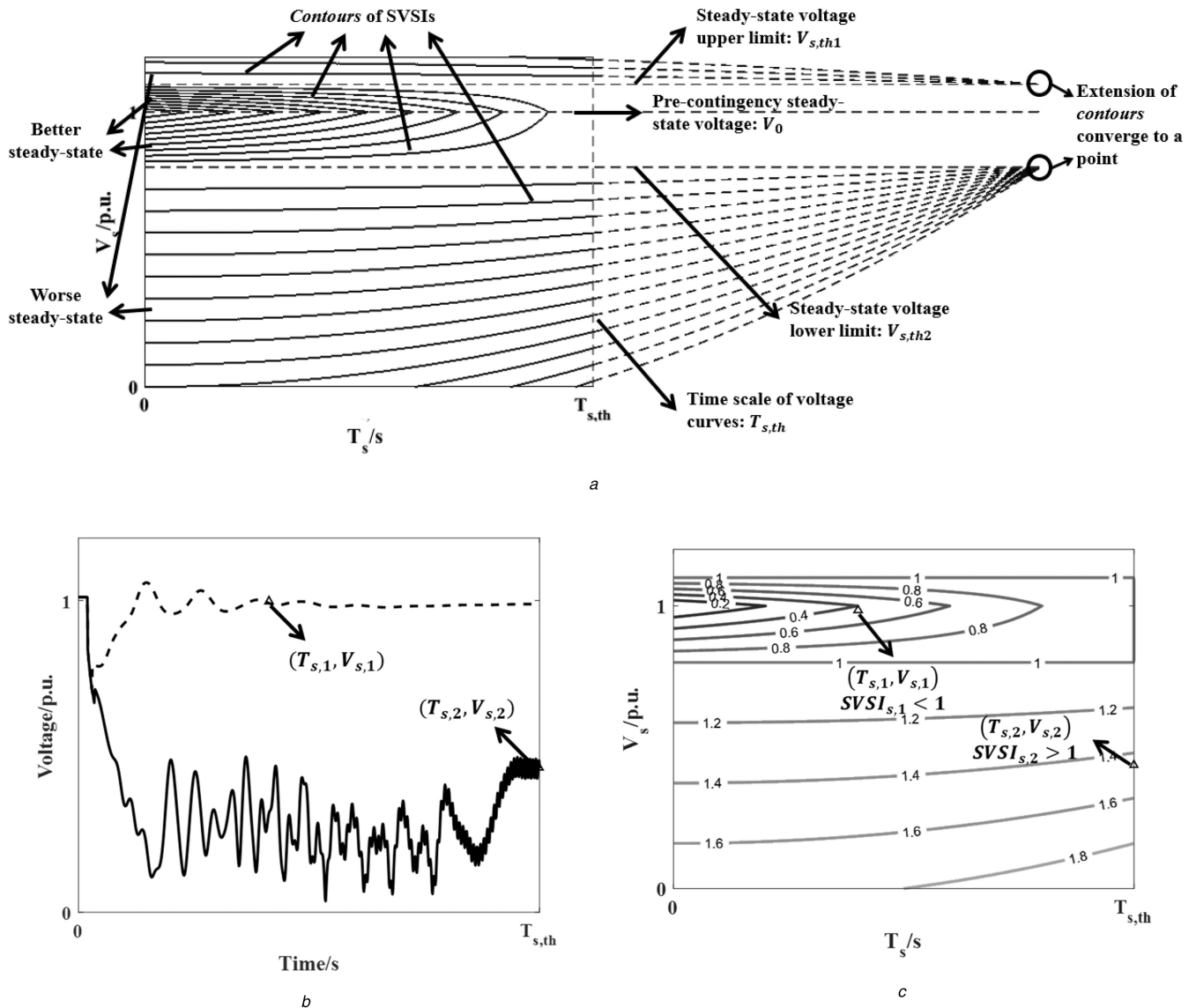


Fig. 4 Schematic of  $SVSI_s$

(a) Schematic of the construction of  $SVSI_s$ , (b) Voltage curves and  $(V_s, T_s)$  under a voltage stable case and a voltage unstable case, (c)  $SVSI_s$  contour and  $(V_s, T_s)$  under a voltage stable case and a voltage unstable case.  $SVSI_s$  is a formula of  $(V_s, T_s)$ , each  $(V_s, T_s)$  that satisfies  $V_s \in (0, +\infty)$  and  $T_s \in (0, 10)$  has a corresponding  $SVSI_s$ . The  $SVSI_s$  of the  $(V_s, T_s)$  in a same blue or black line are same, while the  $SVSI_s$  of the  $(V_s, T_s)$  in different lines are different. The blue lines and black lines are like the contours of  $SVSI_s$ .

and the delay trajectory. If the actual trajectory and the delay trajectory converges, then the trajectory is stable. Otherwise, the trajectory is unstable.

The use of Lyapunov exponents for transient rotor angle stability and SVS analysis is proposed in [30–33]. In particular, an algorithm to calculate the maximum Lyapunov exponent of a single trajectory [32] is shown in (5), which have given us inspiration for construction  $SVSI_l$ . This algorithm considers the voltage curve as a single trajectory

$$\Lambda(k\Delta t) = \frac{1}{Nk\Delta t} \times \sum_{m=1}^N \log \frac{\|V_{(k+m)\Delta t} - V_{(k+m-1)\Delta t}\|}{\|V_{m\Delta t} - V_{(m-1)\Delta t}\|}, \quad k > N \quad (5)$$

$\Delta t$  is the sampling period. For fixed small numbers  $0 < \varepsilon_1 < \varepsilon_2$ ,  $\varepsilon_1 < \|V_{m\Delta t} - V_{(m-1)\Delta t}\| < \varepsilon_2$  is satisfied for  $m = 1, 2, \dots, N$ .  $\Lambda(k\Delta t)$  is the maximum Lyapunov exponent at time  $k\Delta t$ .

Referring to (5), the definition of  $SVSI_l$  is

$$N_l = T_l/T_{spl} \quad (6)$$

$$k_{l\_start} = (T_{end} - T_l)/T_{spl} \quad (7)$$

$$k_{l\_end} = T_{end}/T_{spl} \quad (8)$$

$$SVSI_l = \frac{1}{N_l} \times \sum_{k=k_{l\_start}}^{k_{l\_end}} \frac{1}{N_l k T_{spl}} \times \sum_{m=1}^{N_l} \log \frac{|v((k+m)\Delta t) - v((k+m-1)\Delta t)|}{|v(m\Delta t) - v((m-1)\Delta t)|} \quad (9)$$

$\varepsilon_1 < |v(m\Delta t) - v((m-1)\Delta t)| < \varepsilon_2$  is satisfied for small constants  $0 < \varepsilon_1 < \varepsilon_2$ , and for  $m = 1, 2, \dots, N_l$ .

The  $SVSI_l$  can be regarded as the average value of the maximum Lyapunov exponent defined in (5) from  $T_{end} - T_l$  to  $T_{end}$ .  $T_l$  is the time span for calculating the average maximum Lyapunov exponent. In [32], the author pointed out that if the value of (5) is  $< 0$ , it can be identified that the voltage curve is currently oscillatory stable. Otherwise, it can be identified that the voltage curve is currently oscillatory unstable. Therefore,  $SVSI_l$  indicates the oscillatory status of a voltage curve near  $T_{end}$ , which is also regarded as the oscillatory status of the whole voltage curve in this paper. So if the  $SVSI_l$  of a voltage curve is  $< 0$ , then it can be identified as oscillatory voltage stable. Otherwise, the voltage curve can be identified as oscillatory voltage unstable.

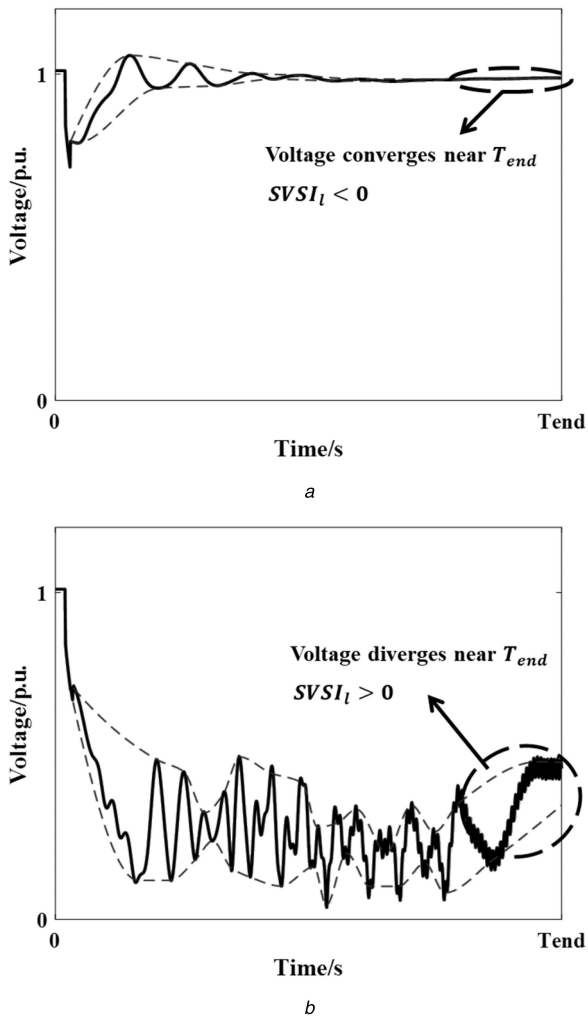


**Fig. 5** Schematic of  $SVSI_l$   
 (a)  $SVSI_l$  under a voltage stable case, (b)  $SVSI_l$  under a voltage unstable case

When  $SVSI_l$  increases, the maximum Lyapunov exponent increases. So the system trajectory tends to diverge, and thus the voltage curve tends to oscillate. When the maximum Lyapunov exponent is 0, it indicates that the convergence of the system trajectory is critical. So when the  $SVSI_l$  is 0, the voltage curve is considered to be critical oscillatory instability. In practical, a voltage oscillation issue will be identified if the oscillation of the voltage curve does not disappear in a short time. Therefore, it is reasonable to identify that the voltage curve is oscillatory unstable if the  $SVSI_l$  is  $> 0$ . So the range of  $SVSI_l$  is  $(-\infty, +\infty)$ . The level of transient voltage oscillation becomes more severe as  $SVSI_l$  increases. When  $SVSI_l$  equals to 0, the level of transient voltage oscillation is critical.

A schematic of  $SVSI_l$  is shown in Fig. 5. The dotted red lines are the envelop curves of the oscillation of the voltage curves. Apparently, the oscillation of the voltage curve is weaker and the damping speed of the voltage curve is quicker in Fig. 5a compared to the oscillation and damping speed of the voltage curve in Fig. 5b. The  $SVSI_l$  of the voltage curve is smaller in Fig. 5a compared to the  $SVSI_l$  of the voltage curve in Fig. 5b. Therefore, the smaller is the value of  $SVSI_l$ , the weaker is the level of oscillation of the voltage curve.

$SVSI_l$  can describe the damping ability of power systems during the transient process, which is closely related to the dynamic responses of high-gain fast-excitation devices [34], the speed control systems of generators [35] and the power system stabilisers (PSSs).

So to decrease  $SVSI_l$  and decrease the level of transient voltage oscillation, we can focus on the modification of the dynamic

control strategies of generators and the performance of PSSs and so on.

## 2.5 Some discussions

After defining the SVSI, we would like to discuss the feasibility, the effectiveness and the future applications of it, which is shown as follows.

First, The SVSI can help in the assessment of a power system threatened by the issues of potential voltage collapse and so on, through quantitatively assessing the result of scanning anticipated contingencies in terms of SVS. By scanning the anticipated contingencies in off-line through numerical simulation, the issue of potential voltage collapse in the power system can be identified. This approach is usually used in the regional power systems of China. The practical application results have shown the feasibility of this approach. However, the current approach requires to manually identify whether the voltage is collapse, thus is inefficient. Moreover, the current approach cannot effectively identify the contingencies that nearly cause a voltage collapse (which are also risky for power systems), thus the potential risk of voltage collapse cannot be fully discovered. However, based on the SVSI, the voltage curves can be quantified assessment, thus can reduce manual work and improve efficiency. Moreover, the SVSI has a threshold, thus it can discover the contingencies which may nearly cause a voltage collapse.

Second, the SVSI is intended to be used in off-line, and to quantitatively assess the SVS of a power system under the anticipated contingencies before the contingencies occurred. Based on the results of scanning the anticipated contingencies of a pre-contingency system, we can further perform preventive control to improve the SVS of the power system. In order to ensure the robustness of the power system, a margin of SVS is usually necessary to be included in the optimisation target of preventive control. The SVSI can not only quantitatively assess the SVS of a power system, but also has a definite threshold, thus it can describe the margin of SVS.

Third, in order to ensure the accuracy of the SVSI in real cases, we mainly calculate the SVSI based on numerical simulation data, thus can avoid the interference from bad data. However, the SVSI is essentially a model-free method, which only based on voltage curves. So actually the SVSI can be calculated based on the phasor measurement unit (PMU) data. However, we have also found out that not only the amount of PMU data is limited, but also the limited data also has problems related to noise, feasible sampling rates, latency in communications and so on. Therefore, we mainly utilise the data from numerical simulation to calculate the SVSI. For the data obtained from numerical simulation, there will not be problems related to noise, feasible sampling rates, latency in communications and so on. Thus, the accuracy of SVSI will not be affected by these issues while implementing in real cases.

Lastly, the SVSI can be possible to address post-contingency topologies to help on system recovery. In the regional power grids of China, usually there is a control strategy map for the anticipated contingencies. The map is generated in off-line. When a contingency occurs on-line, the operators can search for the corresponding preset control strategy in the map. For instance, it is found out that the SVS of the power system can be guaranteed if a certain percentage of load is tripped-off after a certain contingency occurs, then we can preset the control strategy that tripping-off a certain percentage of load when the certain contingency occurs. Based on the SVSI, we can quantitatively assess the effect of control strategies on the SVS of power systems. So the SVSI can guide the generation of the preset control strategies. Additionally, if there is a requirement for the preset control strategies to provide a SVS margin, the SVSI can also be helpful. In order to obtain these preset control strategies, we only require numerical simulation and calculating SVSI in off-line. Therefore, although the SVS is a fast phenomenon, the SVSI can be possible to address post-contingency topologies to help on system recovery.

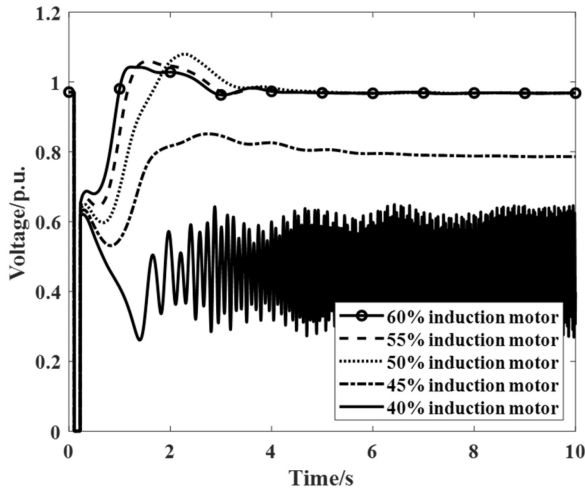


Fig. 6 Voltage curves under different proportion of induction motor loads

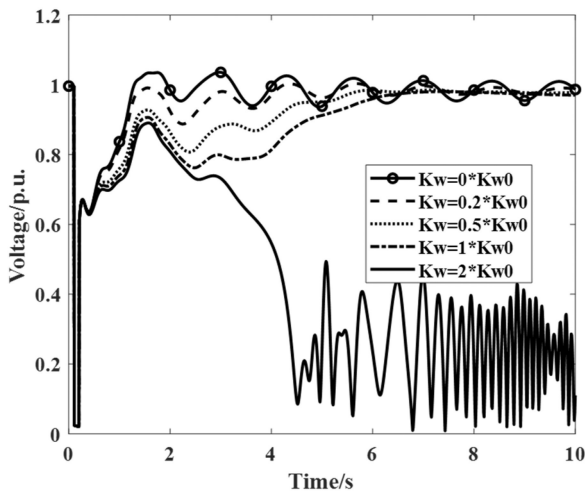


Fig. 7 Voltage curves under different PSS gain

### 3 Verification of the SVSI based on case studies

The verifying case studies are based on the ECPN system model, which contains 3,434 buses, 4630 AC transmission lines, 7 HVDC transmission lines and 423 generators. The ECPN system accepts a large amount of electrical power from external, so it is lack of internal generation equipment. Once the power transmitted through HVDC transmission lines are outage (such as caused by contingencies near HVDC transmission lines), the system will be vulnerable to short-term voltage instability. Therefore, the ECPN system is a typical weak SVS system.

The test cases are mainly based on a typical operating mode in summer. A thorough case study was carried out to verify the effectiveness of SVSI, including modifying proportions of induction motor loads, configurations of PSSs, strategies of under-voltage load-shedding and so on. The contingencies are three-phase short-circuit faults on transmission lines followed by tripping off the fault line, which will be called as three-phase  $N-1$  contingencies in this paper. According to [2], the study period of interest of a SVS problem is in the order of several seconds, so we choose the time duration of 10 s for the case studies in Sections 3 and 4.

The numerical simulation software is PSASP (Power System Analysis Software Package), which is developed by CEPRI (China Electric Power Research Institute). This software is widely used in large region power grids of China (such as the ECPN).

The summarised stability information of the test cases is shown in Table 2. Moreover, the average computational time is much longer for unstable cases compared to the stable cases. Three typical series of the test cases, which modifies the proportion of induction motors, the configurations of PSSs and the strategies of

Table 2 Summary of the test cases

	Stable	Unstable	Total
base case	464	36	500
modify proportion of induction motors	1826	174	2000
modify configurations of PSSs	1794	206	2000
modify strategies of under-voltage load-shedding	1870	130	2000
other cases	4615	385	5000
total	10,569	931	11,500

Table 3 SVSI<sub>r</sub> under different proportion of induction motor loads

Proportion of induction motor	40%	45%	50%	55%	60%
SVSI <sub>r</sub>	0.18	0.655	0.87	1.24	9.895

Table 4 SVSI<sub>l</sub> under different PSS gain

$K_w$	$0 * K_{w0}$	$0.2 * K_{w0}$	$0.5 * K_{w0}$	$1 * K_{w0}$	$2 * K_{w0}$
SVSI <sub>l</sub>	-0.138	-0.300	-0.575	-0.560	0.396

under-voltage load-shedding, respectively, will be presented in detail in this section.

#### 3.1 Case I: SVSI<sub>r</sub> under different proportions of induction motor loads

As stated in Section 2, induction motors can impact the transient voltage restoration and the SVSI<sub>r</sub>. Therefore, this case embodies the effect of SVSI<sub>r</sub> by adjusting the proportion of induction motor loads.  $V_{r,th}$  is 0.7 p.u. and  $T_{r,th}$  is 1 s in this case, since the induction motors near the target bus will stall under the voltage of 0.7 p.u. for 1 s. The  $V_{r,th}$  and  $T_{r,th}$  can be set to different values according to the actual requirements at different buses.

In Fig. 6, the transient restoration ability of voltage curves decreases significantly as the proportion of induction motors increases. When the proportion is 55%, the voltage curve cannot restore to an acceptable voltage level. When the proportion is 60%, the voltage curve is unstable.

In Table 3, the value of SVSI<sub>r</sub> increases significantly as the proportion of induction motors increases. When the proportion is 55%, SVSI<sub>r</sub> is >1, indicating that the voltage curve has a risk of instability. When the proportion is 60%, SVSI<sub>r</sub> is much >1, indicating that the voltage curve is seriously unstable.

As we know, the induction motors will consume massive reactive power at low voltage status. So if we want to improve the transient voltage restoration ability, we can modify the dynamic response of the induction motors to make them more 'friendly' to the transient voltage restoration.

#### 3.2 Case II: SVSI<sub>l</sub> under different configurations of PSSs

As stated in Section 2, PSSs can impact the transient voltage oscillation and the SVSI<sub>l</sub>. Therefore, this case embodies the effect of SVSI<sub>l</sub> by adjusting the parameters of PSSs.  $T_l$  is 1 s and  $T_{spl}$  is 0.01 s in this case. The  $T_l$  and  $T_{spl}$  can be set to different values according to the features of the actual voltage curves.

In Fig. 7, the transient oscillation of voltage curves is weakest when the value of  $K_w$  is moderate. When  $K_w$  equals to  $2 * K_{w0}$ , the voltage curve is unstable. When  $K_w$  equals to 0, the damping speed of the voltage curve is significantly slow.

In Table 4, the value of SVSI<sub>l</sub> is least when the value of  $K_w$  is moderate too. When  $K_w$  equals to  $2 * K_{w0}$ , SVSI<sub>l</sub> is >0, indicating that the voltage curve is divergent/unstable. When  $K_w$  equals to 0, SVSI<sub>l</sub> is much close to 0, indicating that the voltage curve is nearly divergent/unstable.

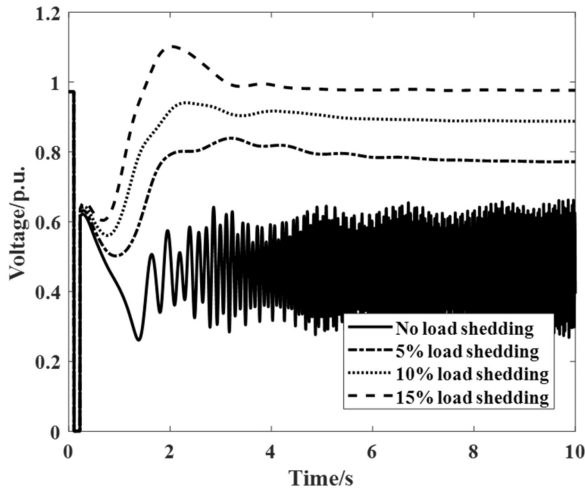


Fig. 8 Voltage curves under different PSS gain

Table 5 SVSI<sub>s</sub> under different strategies of under-voltage load-shedding

Load-shedding ratio	0	5%	10%	15%
SVSI <sub>s</sub>	1.506	1.028	0.760	0.439

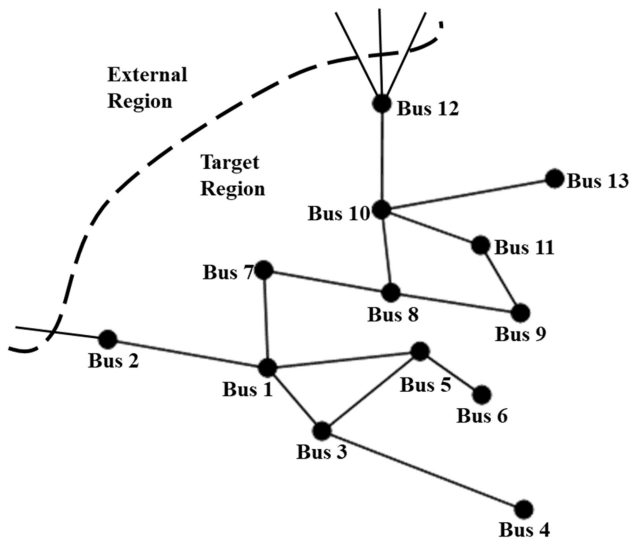


Fig. 9 Single-line diagram of the South Zhejiang power grid

So if we want to mitigate the transient oscillation of the voltage curves, we can reconfigure the PSS parameters to a moderate value.

### 3.3 Case III: SVSI<sub>s</sub> under different strategies of under-voltage load-shedding

As stated in Section 2, under-voltage load-shedding can impact the status of post-contingency steady state and the SVSI<sub>s</sub>. Therefore, this case embodies the effect of SVSI<sub>s</sub> by adjusting the ratios of under-voltage load shedding.  $T_{s,th}$  is 10 s and  $V_{s,th2}$  0.8 p.u., according to [17].  $V_{s,th1}$  is 1.1 p.u., according to [28].  $V_{fluc,th}$  is 0.01 p.u., according to [29]. These parameters can be set to different values according to different operating criteria.

In Fig. 8, the status of post-contingency steady state improves significantly as the ratio of under-voltage load-shedding increases. When the ratio is 10%, the voltage curve can reach an acceptable post-contingency steady state.

In Table 5, the value of SVSI<sub>s</sub> decreases significantly as the ratio of under-voltage load-shedding increases. When the ratio is 10%, SVSI<sub>s</sub> is smaller than 1, indicating that the voltage curve is acceptable in terms of post-contingency steady state.

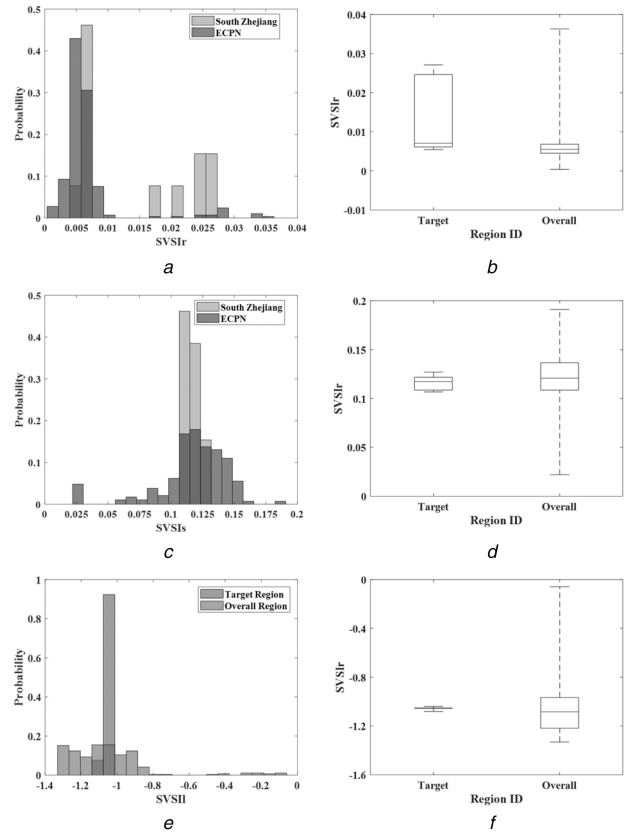


Fig. 10 Comparison of the South Zhejiang region and the ECPN in terms of SVSI

(a), (c), (e) Comparing histogram of SVSI in South Zhejiang region and the ECPN, (b), (d), (f) Comparing boxplot of SVSI in South Zhejiang region and the ECPN

As we know, the reactive power consumed by the loads during the transient process can aggravate the stability of the power system. So cutting off parts of the loads is an effective way to improve voltage stability. In practice, the strategy of cutting off loads includes the under-voltage load-shedding and the under-frequency load-shedding.

## 4 Application of SVSI

In this section, the issue of identifying weak SVS region and searching effective installing locations for dynamic VAR will be analysed and discussed based on SVSI.

The issue of identifying weak SVS region and searching effective installing locations for dynamic VAR can be performed off-line based on numerical simulations. Therefore, SVSI is capable of performing these issues. These two issues are essentially the preliminary steps for the preventive control problems.

According to the operating experiences, the South Zhejiang power grid is a weak SVS region of the ECPN, since it is located at the end of ECPN and connected to the external power grid through only two buses. Additionally, the power generation cannot satisfy the power requirement inside the South Zhejiang power grid, thus require electrical power from external. The single-line diagram of the South Zhejiang power grid is shown in Fig. 9.

In practical, determining weak SVS region is usually based on operating experiences. However, that is laborious and poor in generalisation ability.

In this case, the SVSI will be utilised to quantify the SVS of buses under the anticipated contingencies. By comparing the SVSI of the South Zhejiang region and the whole ECPN, the weakness of South Zhejiang region in terms of SVS can be identified.

This case study is based on a typical operating mode in summer, which is the same as the one in Section 3. The set of anticipated contingencies contains the important three phase  $N-1$  contingencies of the ECPN. The value of the parameters in the definition of SVSI is the same as Section 3. The time duration of simulation is 10 s, which has been explained in Section 3. The

comparison of SVSI in the South Zhejiang region and the whole ECPN is shown in Fig. 10.

In the histograms of Fig. 10, the horizontal axis indicates the component of SVSI, respectively, and the vertical axis indicates the probability of the SVSI component in each value interval. The histograms can be considered as the probability distribution map of each SVSI component. For instance in Fig. 10a, the SVSI<sub>r</sub> in the ECPN are mostly between 0 and 0.01, but a significant part of the SVSI<sub>r</sub> in the South Zhejiang region is around 0.02. Therefore, the profile of SVSI<sub>r</sub> in the South Zhejiang region is greater compared to the profile of SVSI<sub>r</sub> in the ECPN in terms of the histograms.

In the boxplots of Fig. 10, the top and bottom black marks indicate the maximum and minimum value of the SVSI component, respectively. The upper and lower edges of the blue rectangle indicate the 75 and 25% value of the SVSI component, respectively. The central red mark indicates the median value of the SVSI component, respectively. Compared to the histograms, the boxplots contain less information but can better highlight the differences between data. For instance in Fig. 10b, the overall distribution of the SVSI<sub>r</sub> in the South Zhejiang region is greater than the average level of the SVSI<sub>r</sub> in the ECPN. Therefore, the overall level of SVSI<sub>r</sub> in the South Zhejiang region is greater compared to the overall level of SVSI<sub>r</sub> in the ECPN in terms of the boxplots.

So from Fig. 10, the overall level of SVSI<sub>r</sub> in the South Zhejiang region is greater compared to the overall level of SVSI<sub>r</sub> in the ECPN, while the SVSI<sub>s</sub> and SVSI<sub>l</sub> in the South Zhejiang region are both nearly the average level of the SVSI<sub>s</sub> and SVSI<sub>l</sub> in the ECPN. Therefore, the SVS of the South Zhejiang region is weaker than the ECPN, since the overall value of SVSI is greater in the South Zhejiang region.

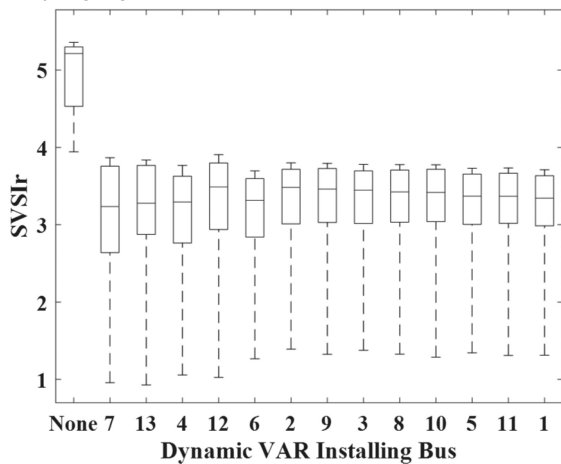


Fig. 11 Boxplot of SVSI<sub>r</sub> under different configurations of dynamic VAR

Moreover, since the difference of the South Zhejiang region and the ECPN in terms of SVSI mainly comes from SVSI<sub>r</sub>, it can be concluded that the SVS problem in the South Zhejiang region mainly stems from the transient voltage restoration issue, which is in consistent with the practical operating experiences. Next, we will evaluate the effect of installing dynamic VAR at different locations based on SVSI, and search for the effective installing locations.

Only the contingencies within the South Zhejiang region are considered in the following case study, since the target is the South Zhejiang region. Moreover, only the SVSI<sub>r</sub> is computed, since the SVS mainly stems from the transient voltage restoration issue. By comparing the overall level of SVSI<sub>r</sub> in the South Zhejiang region when installing the dynamic VAR with the same capacity and parameters in different buses, the most effective installing location for dynamic VAR can be selected. The boxplot of SVSI<sub>r</sub> results are shown in Fig. 11.

The results show that the dynamic VAR can effectively improve the ability of transient voltage restoration in the weak SVS region. By comparing the profile of SVSI<sub>r</sub> under different scenarios, the installing location for dynamic VAR can be chosen according to practical requirements. For instance, if we want to maximise the overall improvement of the SVS, we can choose Bus 7 as the installing location for dynamic VAR. If we want to maximise the improvement of the weakest SVS, we can choose Bus 4 or Bus 6 as the installing location for dynamic VAR. These two results are both reasonable, since Bus 7 is located at the centre of the South Zhejiang region, and the Bus 4 or Bus 6 is located at the end of the South Zhejiang region. Therefore, SVSI can be utilised in searching effective installing locations for dynamic VAR.

## 5 Conclusion

A practical and continuous SVSI based on voltage curves is proposed in this paper. The effectiveness of the proposed index is verified through massive case studies based on ECPN system model.

Three typical verifying cases and one applying case are shown in this paper. The schematic of the main ideas and meanings of the proposed SVSI are presented in Fig. 12. Some features of the SVSI are emphasised as follows.

First, the SVSI is calculated only based on the voltage curves. The voltage curves can be obtained from numerical simulation, PMU measurements and so on. Therefore, the SVSI has a wider applicability compared to the theoretical methods (such as the transient energy function method).

Second, the SVSI is continuous and monotonous, thus it can be used in the optimisation target of the preventive control for improving the SVS of power systems. The optimisation of preventive control is usually performed off-line, and thus the voltage curves can be acquired through numerical simulation. Therefore, the issue of preventive control requires neither PMU

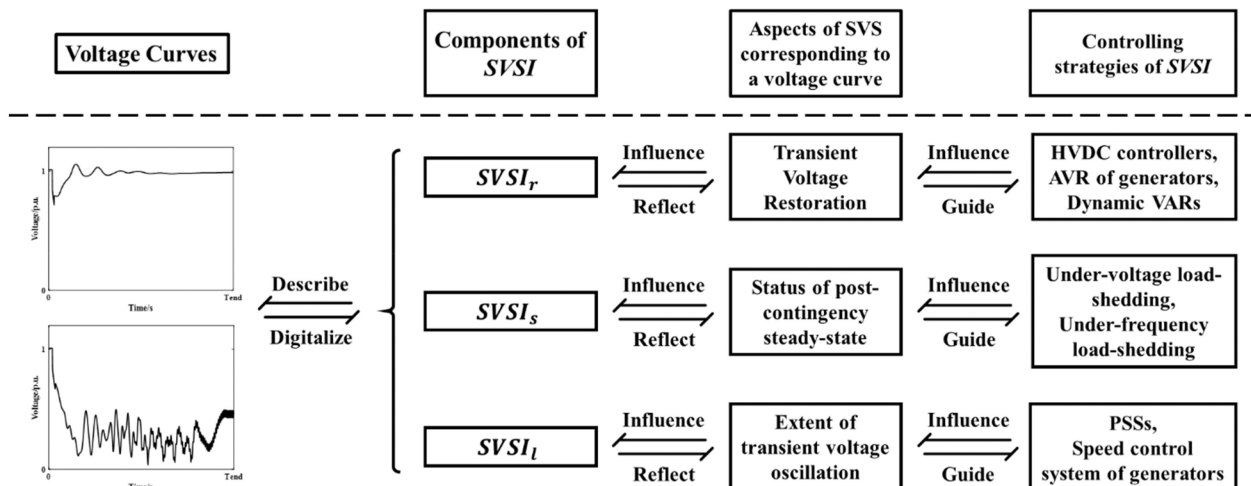


Fig. 12 Schematic of the explanation of SVSI



data nor much computing speed. The SVSI will be mainly used in the preventive control in future works.

Third, the SVSI considers three aspects of the voltage curves in terms of SVS, the weight among them can be modified according to the focus of preventive control. For instance, if the optimisation problem focuses on improving the transient voltage restoration of power systems, the weight of SVSI<sub>1</sub> should be the greatest among the three components.

Lastly, the SVSI realises the digitalisation of voltage curves and can give a comprehensive evaluation of security of SVS, thus it can be used in the practical problems such as identifying weak SVS regions and so on. An application case of SVSI which identifies the weak SVS region of power systems and searches the effective installing locations for dynamic VAR is presented in Section 4.

The conclusions are as follows.

First, the calculation of the SVSI is essentially based on voltage curves, rather than only rely on the result of the numerical simulation. The PMU data can also be used for calculating SVSI, although the accuracy may not be satisfactory. So the SVSI algorithm is robust.

Second, the SVSI is mainly used for off-line analysis. In the regional power grids of China, numerical simulations are usually performed in off-line to identify severe contingencies and to generate the control strategy map. Compared to the current practical SVS criteria/index, the SVSI can give continuous assessment results on the SVS. Therefore, the SVSI can be utilised in the optimisation target of the off-line preventive control for improving the SVS of power systems, and thus can be used in real cases.

Third, the SVSI realises the digitalise of voltage curves in terms of SVS, so there may be potential applications such as clustering of contingencies.

The potential future works are as follows.

First, we will mainly consider the research of preventive control for improving the SVS of power systems utilising SVSI.

Second, we will consider the potential applications of SVSI such as clustering of contingencies.

Third, we will also consider to study the mechanism of stability related to the SVSI, thus enhancing the theoretical basis of the SVSI. For instance, the relation between SVSI and the balance of active power between generators and loads, the damping ability of the power system during the transient process can be part of the future work.

## 6 Acknowledgments

This work is supported by the National Natural Science Foundation for Outstanding Young Scholars (51522702), the National Natural Science Foundation for Innovation Research Group (51621065) and the Technology Project of SGCC ‘Defence and Control of Voltage Process in the AC-DC Interconnected Power System Based on Multiple Data Source and System Development’.

## 7 References

- [1] Potamianakis, E.G., Vournas, C.D.: ‘Short-term voltage instability: effects on synchronous and induction machines’, *IEEE Trans. Power Syst. Trans.*, 2006, **21**, (2), pp. 791–798
- [2] Termsdefinitions, I.J. F.O. S.: ‘Definition and classification of power system stability’, *IEEE Trans. Power Syst.*, 2004, **19**, (2), pp. 1387–1401
- [3] Bo, Z.Q., Lin, X.N., Wang, Q.P., *et al.*: ‘Developments of power system protection and control’, *Protection Control Mod. Power Syst.*, 2016, **1**, (1), p. 7
- [4] Liu, Z., Yu, J., Guo, X., *et al.*: ‘Survey of technologies of line commutated converter based high voltage direct current transmission in China’, *CSEE J. Power Energy Syst.*, 2015, **1**, (2), pp. 1–8
- [5] Tu, J., Zhang, J., Bu, G., *et al.*: ‘Analysis of the sending-side system instability caused by multiple HVDC commutation failure’, *CSEE J. Power Energy Syst.*, 2015, **1**, (4), pp. 37–44
- [6] Wang, C., Yang, L.V., Huang, H., *et al.*: ‘Low frequency oscillation characteristics of east China power grid after commissioning of Huai-Hu ultra-high voltage alternating current project’, *J. Mod. Power Syst. Clean Energy*, 2015, **3**, (3), pp. 332–340
- [7] Fouad, A., Vittal, V.: ‘Power system response to a large disturbance: energy associated with system separation’, *IEEE Trans. Power Appa. Syst.*, 1983, **102**, (11), pp. 3534–3540
- [8] Llamas, A., De, L.R.L.J., Mili, L., *et al.*: ‘Clarifications of the BCU approach for transient stability analysis’, *IEEE Trans. Power Syst.*, 1995, **10**, (1), pp. 210–219
- [9] Xue, Y., Van Cutsem, T., Ribbens-Pavella, M.: ‘Extended equal area criterion justifications, generalizations, applications’, *IEEE Trans. Power Syst. Trans.*, 1989, **4**, (1), pp. 44–52
- [10] Yu Yixin, A.: ‘Study on dynamic security regions of power systems’. Proc. Electric Power System and Automation, Siem Reap, Cambodia, June 1990
- [11] Yang, X., Jin, Y.X., Chen, Y.: ‘Stability analysis of AC/DC power transmission system based on bifurcation theories’. Int. Conf. Sustainable Power Generation and Supply, 2009. SUPERGEN ‘09, Chengdu, China, March 2009, pp. 1–7
- [12] Ma, Y.J., Li, X.S., Zhou, X.S., *et al.*: ‘The comments on dynamic bifurcation of voltage stability in power system’. Wase Int. Conf. Information Engineering. IEEE Computer Society, Beidaihe, Hebei, China, August 2010, pp. 272–275
- [13] NERC Planning Standards: Available at <http://www.nerc.com>
- [14] NERC/WECC: ‘Planning standards’, 2003, Available at <https://www.wecc.biz>
- [15] TVA: ‘TVA 2003 transient stability planning criteria’, 2003, Available at <https://www.tva.gov/>
- [16] National Energy Board: ‘Technique specification of power system security and stability calculation’ (China Electric Power Press, Beijing, China, 2013)
- [17] SGCC. Q / GDW 404–2010: ‘Security and stability of the national grid computing specification’ (China Electric Power Press, Beijing, China, 2010)
- [18] CSG. Q / CSG 11004–2009: ‘Guide on security and stability analysis for CSG’. 2009
- [19] Overbye, T.J., Klump, R.P.: ‘Determination of emergency power system voltage control actions’, *IEEE Trans. Power Syst.*, 1998, **13**, (1), pp. 205–210
- [20] Capitanescu, F., Van Cutsem, T.: ‘Preventive control of voltage security margins: a multicontingency sensitivity-based approach’, *IEEE Trans. Power Syst.*, 2002, **17**, (2), pp. 358–364
- [21] Vaahedi, E., Mansour, Y., Fuchs, C., *et al.*: ‘Dynamic security constrained optimal power flow/Var planning’, *IEEE Trans. Power Syst.*, 2001, **16**, (1), pp. 38–43
- [22] Xu, Y., Dong, Z.Y., Meng, K., *et al.*: ‘Multi-objective dynamic VAR planning against short-term voltage instability using a decomposition-based evolutionary algorithm’, *IEEE Trans. Power Syst.*, 2014, **29**, (6), pp. 2813–2822
- [23] Xu, Y., Zhang, R., Zhao, J., *et al.*: ‘Assessing SVS of electric power systems by a hierarchical intelligent system’, *IEEE Trans. Neural Netw. Learn. Syst.*, 2015, **27**, (8), pp. 1–1
- [24] Dong, Y., Xie, X., Zhou, B., *et al.*: ‘An integrated high side var-voltage control strategy to improve SVS of receiving-end power systems’, *IEEE Trans. Power Syst.*, 2015, **31**, (3), pp. 1–11
- [25] Wildenhues, S., Rueda, J.L., Erlich, I.: ‘Optimal allocation and sizing of dynamic VAR sources using heuristic optimization’, *IEEE Trans. Power Syst.*, 2014, **30**, (5), pp. 1–9
- [26] Paramasivam, M., Salloum, A., Ajarapu, V., *et al.*: ‘Dynamic optimization based reactive power planning to mitigate slow voltage recovery and short term voltage instability’, *IEEE Trans. Power Syst.*, 2013, **28**, (4), pp. 3865–3873
- [27] Tiwari, A., Ajarapu, V.: ‘Optimal allocation of dynamic var support using mixed integer dynamic optimization’, *IEEE Trans. Power Syst.*, 2011, **26**, (1), pp. 305–314
- [28] Standardization Administration of the People's Republic of China, GB/t 12325–2008: ‘Power quality – deviation of supply voltage’, China Electric Power Press, Beijing, 2008
- [29] China Machinery Industry Standard, (CMIS), GB/t 12326–2008: ‘Power quality – voltage fluctuation and flicker’, 2008
- [30] Liu, C.W., Thorp, J.S., Lu, J., *et al.*: ‘Detection of transiently chaotic swings in power systems using real-time phasor measurements’, *IEEE Trans. Power Syst. Pwrs.*, 1994, **9**, (3), pp. 1285–1292
- [31] Yan, J., Liu, C.C., Vaidya, U.: ‘PMU-based monitoring of rotor angle dynamics’, *IEEE Trans. Power Syst.*, 2011, **26**, (4), pp. 2125–2133
- [32] Dasgupta, S., Paramasivam, M., Vaidya, U., *et al.*: ‘Real-time monitoring of short-term voltage stability using PMU data’, *IEEE Trans. Power Syst.*, 2013, **28**, (4), pp. 3702–3711
- [33] Ge, H., Guo, Q., Sun, H., *et al.*: ‘An improved real-time short-term voltage stability monitoring method based on phase rectification’, *IEEE Trans. Power Syst.*, 2017, **PP**, (99), pp. 1–1
- [34] Brown, P.G., Demello, F.P., Lenfest, E.H., *et al.*: ‘Effects of excitation, turbine energy control, and transmission on transient stability’, *IEEE Trans. Power Appar. Syst.*, 1970, **PAS-89**, (6), pp. 1247–1252
- [35] Vournas, C.D.: ‘Unstable frequency oscillations in a slow-response reheat-turbine generator’. IEEE Power Engineering Society 1999 Winter Meeting, New York, NY, USA, 31 January - 4 February 1999, vol. 1, pp. 140–144